Electrokinetic Control of Viscous Fingering

Mohammad Mirzadeh[1] and Martin Z. Bazant[1,2,*]
[1]Department of Chemical Engineering, Massachusetts Institute of Technology, Cambridge, Massachusetts 02139, USA
[2]Department of Mathematics, Massachusetts Institute of Technology, Cambridge, Massachusetts 02139, USA
(Received 19 June 2017; published 26 October 2017)

We present a theory of the interfacial stability of two immiscible electrolytes under the coupled action of pressure gradients and electric fields in a Hele-Shaw cell or porous medium. Mathematically, our theory describes a phenomenon of "vector Laplacian growth," in which the interface moves in response to the gradient of a vector-valued potential function through a generalized mobility tensor. Physically, we extend the classical Saffman-Taylor problem to electrolytes by incorporating electrokinetic (EK) phenomena. A surprising prediction is that viscous fingering can be controlled by varying the injection ratio of electric current to flow rate. Beyond a critical injection ratio, stability depends only upon the relative direction of flow and current, regardless of the viscosity ratio. Possible applications include porous materials processing, electrically enhanced oil recovery, and EK remediation of contaminated soils.

DOI: 10.1103/PhysRevLett.119.174501

Interfacial instability is the precursor to pattern formation in a variety of physical and chemical processes [1,2]. This fascinating topic covers a broad range of phenomena such as dendritic growth due to the Mullins-Sekerka instability in solidification [3,4], fractal growth due to diffusion-limited aggregation [5] or metal electrodeposition [6] in fluid flows [7], crease formation and wrinkling of combustion fronts due to the Darrieus-Landau instability [8,9], and viscous fingering in Hele-Shaw cells [10] and porous media [11] due to the Saffman-Taylor instability [12,13].

Interfacial instabilities are usually undesirable, but difficult to control. In secondary oil recovery, viscous fingering of injected liquids leads to nonuniform displacement and residual trapping of oil [11,14], and dendritic growth is a major safety concern for metal anodes in rechargeable batteries [15]. There are signs, however, that instability may be avoided if the interface is driven by multiple opposing forces. For instance, it was recently observed that dendritic growth can be suppressed in charged porous media [16] if preceded by deionization shock wave [17], whose stable propagation in cross flow also enables water purification by shock electrodialysis [18,19].

Here, we consider the interfacial stability of two immiscible electrolytes in a Hele-Shaw cell where the interface is set into motion by both the pressure-driven and electro-osmotic flows. Remarkably, we find that electrokinetic (EK) coupling influence interfacial stability and, under certain conditions, can eliminate viscous fingering. This phenomenon illustrates the rich physics of "vector Laplacian growth" (VLG), a general mathematical model of interfacial dynamics driven by the gradient of a vector-valued potential function through a generalized mobility tensor. The "one-sided" VLG model (with field gradients only on one side of the interface) is known to be unstable, leading to fractal patterns, during growth [7] and stable, resulting in smooth collapse, during retreat [20,21]. Our theory shows that stable growth is also possible, if field gradients exist on both sides of the interface.

In the classical viscous fingering problem, the fluid flow in a Hele-Shaw cell can be approximated as quasi-two-dimensional if the cell gap, b, is much smaller than the lateral dimension, L (see Fig. 1). In this case, the gap-averaged velocity of each fluid is given by

$$\mathbf{u}^{\pm} = -\frac{b^2}{12\mu^{\pm}}\nabla p^{\pm}, \qquad \nabla\cdot\mathbf{u}^{\pm} = 0, \tag{1}$$

where "−" and "+" superscripts denote invading and receding fluids, μ and p are viscosity and pressure of each fluid, and ∇ is the in-plane gradient operator. At the

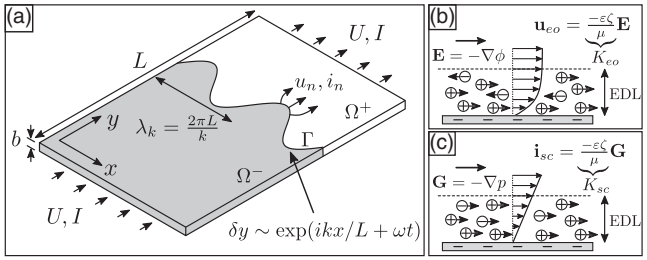

FIG. 1. Schematic of flow in a rectangular Hele-Shaw cell. (a) The interface (Γ) between two immiscible electrolytes moves under the coupled action of pressure gradient and electric field as described by the EK response of the cell. (b) In addition to the pressure-driven flow, the electric field exerts a net force on ions in the electric double layer (EDL), resulting in the electro-osmotic flow. (c) Similarly, in addition to the Ohmic current driven by the electric field, the pressure-driven flow advects charges in the EDL, resulting in the streaming current.

interface, the pressure jump is given by the Young-Laplace equation, while the normal velocity is continuous,

$$[\![p]\!] = \gamma\kappa, \qquad [\![\hat{\mathbf{n}} \cdot \mathbf{u}]\!] = 0, \tag{2}$$

where $[\![a]\!] \equiv a^+ - a^-$ denotes the jump of variable a across the interface, γ is the surface tension, and κ is the in-plane curvature. More generally, these conditions must be modified to take the finite lubrication film thickness into account if the receding fluid is perfectly wetting [11,22]. The interface moves with the local fluid velocity,

$$\frac{d\mathbf{x}}{dt} = (\hat{\mathbf{n}} \cdot \mathbf{u})\hat{\mathbf{n}}, \tag{3}$$

and the far-field flow is uniform.

Linear stability analysis of Eqs. (1)–(3), initiated by Chuoke *et al.* [13] and Saffman and Taylor [12], reveals that stable displacement is only possible if the advancing fluid is more viscous,

$$\text{Stable}: M = \frac{\mu^-}{\mu^+} > 1. \tag{4}$$

In the opposite case, $M < 1$, the interface is unstable to perturbations of sufficiently long wavelength, and the less viscous fluid forms "fingers" of lower resistance through the more viscous fluid. Specifically, the growth rate, ω, of a normal mode $\delta y \sim \exp(ikx/L + \omega t)$ satisfies the dispersion relation [10,11]

$$\omega = \frac{k}{L}\left(U\frac{\mu^+ - \mu^-}{\mu^+ + \mu^-} - \frac{\gamma b^2 k^2}{12L^2(\mu^+ + \mu^-)}\right), \tag{5}$$

where k is the wave number. Perturbation wavelengths longer than $\lambda_{\text{cr}} = \pi b\sqrt{\gamma/3U(\mu^+ - \mu^-)}$ are unstable, and the maximum growth rate arises for $\lambda_m = \sqrt{3}\lambda_{\text{cr}}$.

Most materials naturally acquire charge in aqueous solutions from the dissociation of surface groups, such as silanol [23,24], for glass in Hele-Shaw cells or silicate minerals in underground reservoirs. The screening of surface charge by mobile ions leads to the formation of electric double layers (EDLs) and associated EK phenomena [25]. An electric field parallel to the charged surface acts on EDL charge to drive "electro-osmotic" flow $\mathbf{u}_{\text{eo}}$, while pressure-driven flow drives "streaming current" $\mathbf{i}_{\text{sc}}$ due to the advection of EDL charge (Fig. 1). For typical situations of fixed surface charge, the EK response is linear in the driving forces, i.e., $\mathbf{u}_{\text{eo}} = -K_{\text{eo}}\nabla\phi$ and $\mathbf{i}_{\text{sc}} = -K_{\text{sc}}\nabla p$, where ϕ is the electrostatic potential. The electro-osmotic mobility, K_{eo}, and the streaming conductance, K_{sc}, satisfy Onsager's reciprocal relation [26,27], $K_{\text{eo}} = K_{\text{sc}}$, and for thin EDL (gaps, $b \sim 0.1$–1mm, much larger than the EDL thickness, $\lambda_D \sim 1$–10 nm), are given by the Helmholtz-Smoluchowski relation [25], $K_{\text{eo}} = -\varepsilon\zeta/\mu$, where ε is the electrolyte permittivity and ζ is the potential difference across the EDL [24,25].

When linear EK phenomena are considered, a VLG model can thus be written in terms of a tensorial flux, $\mathbf{F} = (\mathbf{u}, \mathbf{i})^{\mathsf{T}}$, proportional to the gradient of a vector-valued potential, $\mathbf{\Phi} = (p, \phi)^{\mathsf{T}}$,

$$\mathbf{F}^{\pm} = -\mathbb{K}^{\pm}\nabla\mathbf{\Phi}^{\pm}, \qquad \nabla \cdot \mathbf{F}^{\pm} = \mathbf{0}, \tag{6}$$

where $\mathbb{K}$ is the EK mobility tensor,

$$\mathbb{K} = \begin{pmatrix} K_h & K_{\text{eo}} \\ K_{\text{eo}} & K_e \end{pmatrix}. \tag{7}$$

$K_h = b^2/12\mu$ is the hydraulic Darcy conductivity, and $K_e = \sigma$ is the electrical Ohmic conductivity of the cell. The second law of thermodynamics requires positive definite $\mathbb{K}$ to ensure positive dissipation rate [28,29], i.e.,

$$-\nabla\mathbf{\Phi} \cdot \mathbf{F} = \nabla\mathbf{\Phi}^{\mathsf{T}}\mathbb{K}\nabla\mathbf{\Phi} > 0. \tag{8}$$

At the interface, the pressure and total velocity satisfy the jump conditions given by Eq. (2), while the potential and normal component of the total current are continuous, which can be compactly expressed as

$$[\![\mathbf{\Phi}]\!] = (\gamma\kappa, 0)^{\mathsf{T}}, \qquad [\![\hat{\mathbf{n}} \cdot \mathbf{F}]\!] = \mathbf{0}. \tag{9}$$

Far from the interface in a planar geometry, the fluxes are assumed to be uniform, $\lim_{y\to\pm\infty}\mathbf{F}_y = \mathbf{F}_\infty = (U, I)^{\mathsf{T}}$. Equations (6) and (9), along with the kinematic condition (3), determine the interface motion.

As for classical problem, we consider the linear stability of a planar interface subjected to a sinusoidal perturbation, $\delta y \sim \exp(ikx/L + \omega t)$, and seek solutions of the form $\mathbf{\Phi}^{\pm} = \mathbf{\Phi}_0^{\pm} + \epsilon\mathbf{\Phi}_1^{\pm}$ in the limit of $\epsilon \ll 1$. From Eq. (6), the base state is linear, i.e., $\mathbf{\Phi}_0^{\pm} = -\mathbb{K}^{\pm^{-1}}\mathbf{F}_\infty(y - Ut)$, while $\mathbf{\Phi}_1^{\pm} = \mathbf{A}_1^{\pm}\exp(ikx/L + \omega t)\exp[\mp k(y - Ut)/L]$, where $\mathbf{A}_1^{\pm}$ are evaluated using the jump condition (9). Applying the kinematic condition (3) then yields the growth rate

$$\omega = \frac{k}{L}\left(F - \gamma G\frac{k^2}{L^2}\right), \tag{10}$$

where F and G are given by

$$\begin{aligned} F &= U\frac{[\![K_{\text{eo}}]\!]\{K_{\text{eo}}\} - [\![K_h]\!]\{K_e\}}{\det\{\mathbb{K}\}} \\ &\quad + 2I\frac{K_h^+K_{\text{eo}}^- - K_h^-K_{\text{eo}}^+}{\det\{\mathbb{K}\}}, \\ G &= \frac{K_h^+\det\mathbb{K}^- + K_h^-\det\mathbb{K}^+}{\det\{\mathbb{K}\}}, \end{aligned} \tag{11}$$

and $\{a\} \equiv a^+ + a^-$. Note that the classical dispersion relation (5) is recovered in the absence of EK phenomena, $K_{\text{eo}}^{\pm} = 0$. From the Second Law (8), it follows that $G > 0$,

ensuring that surface tension effects are stabilizing. Therefore, $F < 0$ is a sufficient condition for stability. For $F > 0$, a perturbation of wavelength longer than $\lambda_{cr} = 2\pi\sqrt{\gamma G/F}$ is unstable, and $\lambda_m = \sqrt{3}\lambda_{cr}$ is the most unstable wavelength.

To simplify Eq. (11), we note that the EK coupling coefficient [30], $\alpha = K_{eo}^2/K_h K_e$, is typically small, while $0 \le \alpha < 1$ from Eq. (8). For $\alpha \ll 1$, the critical wavelength may be approximated as

$$\lambda_{cr} = \pi b \sqrt{\frac{\gamma}{3U[\![\mu]\!] + 6I[\![\varepsilon\zeta]\!]/\{\sigma\}}}. \tag{12}$$

While the classical instability is controlled by the viscosity ratio [Eq. (4)], our theory predicts that the injection ratio, I/U, can be tuned independently to control interfacial stability [Fig. 2(a)],

$$\text{Stable:}\ \frac{M-1}{M+1} > A\frac{SZ-1}{SZ+1}, \tag{13}$$

in terms of the following dimensionless ratios:

$$S = \frac{\varepsilon^-}{\varepsilon^+}, \quad Z = \frac{\zeta^-}{\zeta^+}, \quad M = \frac{\mu^-}{\mu^+}, \quad A = \frac{I(-\overline{\varepsilon\zeta})}{U\bar{\mu}\,\bar{\sigma}}, \tag{14}$$

where the over-bar indicates average values, e.g., $\overline{\varepsilon\zeta} = (\varepsilon^+\zeta^+ + \varepsilon^-\zeta^-)/2$. EK effects require $SZ \neq 1$, and stability is possible if the injection ratio is larger than $|(M-1)(SZ+1)/(SZ-1)(M+1)|$, and has the "correct" sign, depending on the magnitude of SZ (see Fig. 2). Above a critical injection ratio, $A_{cr} = |(SZ+1)/(SZ-1)|$, stability is entirely determined by the sign of injection ratio and is, remarkably, independent of the viscosity ratio. Physically, negative injection ratios denote opposite direction of current and flow. These observations are illustrated in Figs. 2(b)–2(d).

Motivated by secondary oil recovery, it is interesting to consider the limit when $M \ll 1$, $SZ \gg 1$, and $R = \sigma^-/\sigma^+ \gg 1$, e.g., when water is pushing oil toward extraction wells. In this case, negative current injection shifts the critical wavelength to longer values and reduces viscous fingering. Stable displacement is possible if $I > I_{cr}$, where

$$I_{cr} \approx \frac{U}{2}\frac{\mu^o}{\mu^w}\frac{\sigma^w}{K_{eo}^w}. \tag{15}$$

For $U = 1$ mm/min in a 1 mM KCl solution with $\zeta = -50$ mV and $\mu^w/\mu^o = 0.1$, the critical current is fairly small, $I_{cr} \sim 4$ mA/cm^2, but a large critical electric field is required to drive this current across the poorly conducting oil region,

$$E_{cr} \approx \frac{U}{4}\frac{\mu^o}{\mu^w}\frac{\sigma^w}{\sigma^o}\frac{1}{K_{eo}^w}. \tag{16}$$

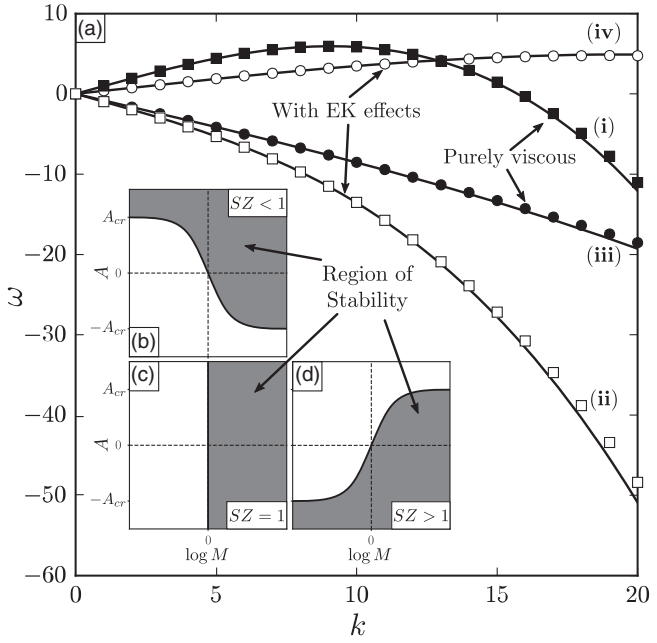

FIG. 2. Linear stability analysis of a planar interface. (a) The nondimensional growth rate ω (scaled with U/L) versus the wave number k. Solid lines represents the theory [see Eq. (10)] while symbols are numerically computed growth rates, obtained by evolving a small-amplitude initial perturbation ($\epsilon = 10^{-3}$) for each wave number. Shown are classical results (no EK effects) for (i) unfavorable ($M = 0.01$) and (iii) favorable ($M = 10$) viscosity ratios. When EK effects are present, stability can be manipulated by adjusting the injection ratio, resulting in either (ii) suppression of viscous fingering ($M = 0.01$, $SZ = R = 100$, $A \approx -1.98$), or (iv) EK fingering ($M = SZ = R = 10$, $A \approx 1.45$). Here, $R = \sigma^-/\sigma^+$ is the conductivity ratio and the remaining parameters are defined via Eq. (14). In all cases, the effective capillary number, $\mathrm{Ca} = 12L^2U\mu^+/\gamma b^2$, is set to 250. (b)–(d) The shaded area illustrates the region of stability as approximated by Eq. (13). Interestingly, this region is symmetrical around $SZ = 1$, for which classical results are recovered.

Even for a modest value of $\sigma^w/\sigma^o = 10$, complete suppression of viscous fingering requires $E_{cr} \sim 150$ V/cm. The required voltage could be lowered by reducing the conductivity ratio or electrode separations. Nonetheless, partial stabilization (with enhanced oil recovery) is still viable with electric fields below the critical value.

To further support our theory, we numerically solve the VLG model using the Voronoi Interface Method [31] to discretize the conservation equations (6) subjected to the interface jump conditions (9) while utilizing the level-set framework [32] to represent the moving interface. Furthermore, we use dynamically adaptive quadtree grids [33] as well as parallel algorithms [34] for fast and high-fidelity simulations. Figure 3 illustrates the interfacial dynamics of an initial perturbation for unfavorable, Figs. 3(a) and 3(b), and favorable, Figs. 3(c) and 3(d), viscosity ratios. As predicted, interfacial stability can be manipulated by adjusting the injection ratio.

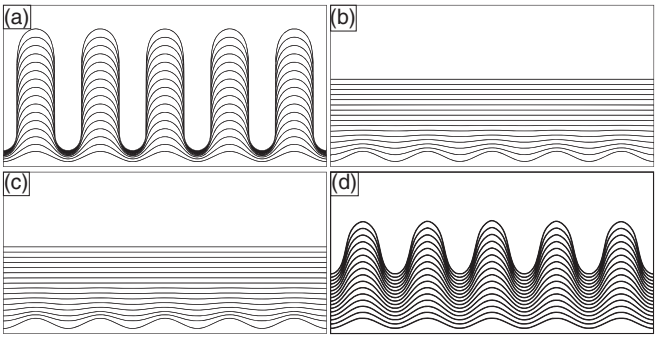

FIG. 3. Numerical simulation of the interfacial dynamics for an initial perturbation. The interface moves upward and its location is drawn at equal time intervals. (a) Viscous fingering for an unfavorable viscosity ratio $M = 0.01$ and (b) its suppression using negative injection ratio [same parameters as in Fig. 2(a), line (ii)]. (c) Stable displacement for favorable viscosity ratio $M = 10$ and (d) formation of EK fingering with positive injection ratio [same parameters as in Fig. 2(a), line (iv)].

It is straightforward to extend the analysis for the radial Hele-Shaw cell geometry [11,35] where an invading fluid is injected at a point to push the second fluid outward. If the interface is initially assumed to be circular, the growth rate of an azimuthal perturbation of the form $\delta r \sim \exp(ik\theta + \omega t)$, is given via

$$\omega = -\frac{U}{r} + \frac{k}{r}\left(F - \gamma G \frac{(k^2-1)}{r^2}\right), \tag{17}$$

where r is the initial radius and F and G are still given by Eq. (11). Once again, $F < 0$ is a sufficient condition for stability. Therefore, the stability estimate in Eq. (13) could be used in radial geometry if velocity, U, and current density, I, are replaced by the total flow rate, Q_0, and total current, I_0, respectively. Figure 4 illustrates numerical simulation of interface evolution in a radial Hele-Shaw cell geometry for an unstable viscosity ratio of $M = 0.01$. The instability is entirely suppressed when current is injected in the opposite direction.

The possibility of manipulating interfacial instabilities is quite exciting. The idea of controlling viscous fingering using cell geometry has been recently discussed [36], and our framework introduces many other degrees of freedom, such as the placement of electrodes, dielectric or conducting boundaries, and surface coatings or gate voltages to modify local zeta potentials. For a given geometry, dynamical control of fingering instabilities may also be possible, by adjusting potentials and pressures with real-time feedback from currents and flow rates.

Hele-Shaw cell experiments could be used to check these predictions and test the validity of our assumptions. Since EK phenomena depend on which liquid is in contact with the surface, it may be necessary to extend the model for lubrication films and gravity currents [37], which would require more complicated depth-averaging and EKs at the

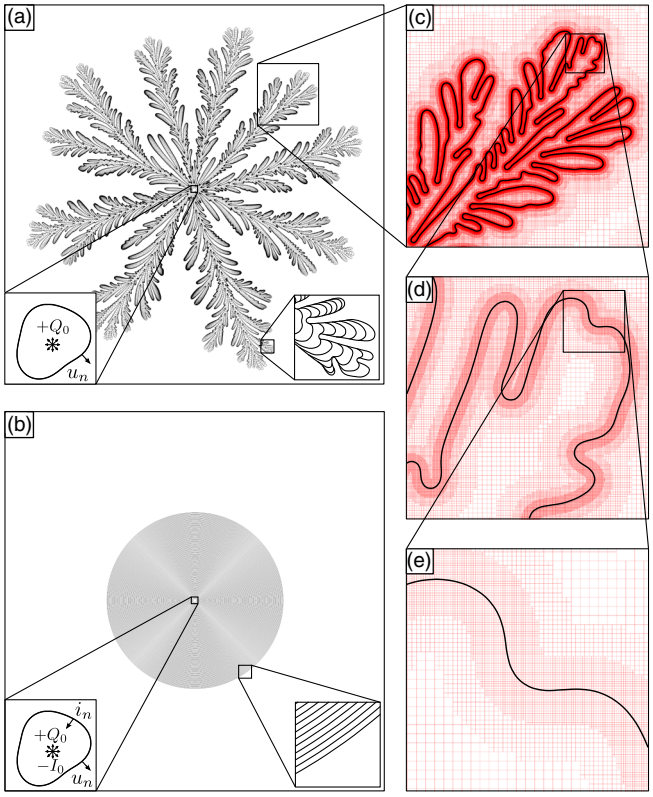

FIG. 4. Numerical simulation of the interfacial dynamics in a radial Hele-Shaw cell. (a) An initial "bubble" (left inset) separates two immiscible ($M = 0.01$) and grows outward due to a positive flow source in the middle. The interface location, drawn at equal time intervals (right inset), reveals a complex pattern due to successive growth and tip-splitting. (b) The viscous fingering is entirely suppressed by injecting electric current in the opposite direction, resulting in a uniform circular growth [same parameters as in Fig. 2(a), line (ii)]. (c)–(e) Snapshot of the final pattern in (a), illustrating the level of detail that is captured in the simulation.

liquid-liquid interface [38], perhaps amenable to conformal-map dynamics [7,39]. We have also neglected nonlinear electrohydrodynamic effects [40] which might cause interfacial instabilities at higher electric fields in large channels [41–43]. We also assume finite electrical resistance in each phase, which could exclude traditional liquid pairs, such as water-silicon oil and air-glycerol pairs, although some poorly conducting regions may have sufficient ionic or electronic conductivity to pass at least a transient current consistent with the model. The model could be extended to include interfacial capacitance, and the resulting "*RC* time" for charge accumulation might be longer than the instability growth time, especially for large resistive domains.

Our model is directly applicable to interfaces between two immiscible electrolyte solutions (ITIES) that support charge-transfer reactions [44]. Examples include aqueous electrolytes, e.g., LiCl, in contact with solutions of lipophilic salts in organic solvents, e.g., tetrabutylammonium

tetraphenylborate (TBATPB) in nitrobenzene [45]. Recent interest in ITIES was spurred by electro-wetting [46] for electrovariable optics [47], but tunable fingering under confinement could lead to different applications.

Although our theory is for immiscible electrolytes, it may also describe diffuse interfaces involving strong ion concentration gradients, e.g., deionization shocks in charged porous media [17] or pH fronts in EK remediation of contaminated soil [48]. Since the ζ potential is a function of pH and salt concentration [23,24], it may also be possible to observe some of the stabilizing effects with miscible solutions, perhaps in charged porous media such as glass frit or Hele-Shaw cells packed with silica beads. Finally, we caution that viscous fingering is more complicated in porous media than in Hele-Shaw cells, due to permeability variations, capillary effects, and surface wettability [49,50]. Since EK couplings derive from surfaces, we expect strong dependence on surface wettability whereas permeability variations might have limited impact due to disproportionate scaling of hydraulic and electroosmotic mobilities with the pore size, possibly resulting in a more uniform displacement. Nonetheless, further investigation is required to quantify the degree to which EK phenomena can control interfacial stability in porous media.

The authors thank Amir A. Pahlavan and Charles W. Monroe for useful discussions. This work was supported by a seed grant from the Massachusetts Institute of Technology Energy Initiative with computational resources from the Texas Advanced Computing Center (TACC) at The University of Texas at Austin and the Extreme Science and Engineering Discovery Environment (XSEDE), supported by Grant No. ACI-1548562 from the National Science Foundation.

*bazant@mit.edu

[1] D. A. Kessler, J. Koplik, and H. Levine, Adv. Phys. **37**, 255 (1988).
[2] P. Pelcé and A. Libchaber, *Dynamics of Curved Fronts* (Elsevier, New York, 2012).
[3] W. W. Mullins and R. F. Sekerka, J. Appl. Phys. **34**, 323 (1963); **35**, 444 (1964).
[4] J. Langer, Rev. Mod. Phys. **52**, 1 (1980).
[5] T. A. Witten and L. M. Sander, Phys. Rev. B **27**, 5686 (1983).
[6] R. Brady and R. Ball, Nature (London) **309**, 225 (1984).
[7] M. Z. Bazant, J. Choi, and B. Davidovitch, Phys. Rev. Lett. **91**, 045503 (2003).
[8] G. Darrieus, in La Technique Moderne, 1938 (unpublished); in Congrès de Mécanique Appliquée, 1945 (unpublished); L. Landau, Acta Physicochim. URSS **19**, 77 (1944).
[9] G. I. Sivashinsky, Annu. Rev. Fluid Mech. **15**, 179 (1983); M. Matalon, Annu. Rev. Fluid Mech. **39**, 163 (2007).
[10] D. Bensimon, L. P. Kadanoff, S. Liang, B. I. Shraiman, and C. Tang, Rev. Mod. Phys. **58**, 977 (1986).
[11] G. M. Homsy, Annu. Rev. Fluid Mech. **19**, 271 (1987).
[12] P. G. Saffman and G. Taylor, Proc. R. Soc. A **245**, 312 (1958).
[13] R. Chuoke, P. Van Meurs, and C. van der Poel, *Petroleum Transactions, AIME*, Vol. 216 (1959), pp. 188–194.
[14] S. B. Gorell and G. Homsy, SIAM J. Appl. Math. **43**, 79 (1983).
[15] W. Xu, J. Wang, F. Ding, X. Chen, E. Nasybulin, Y. Zhang, and J.-G. Zhang, Energy Environ. Sci. **7**, 513 (2014).
[16] J.-H. Han, M. Wang, P. Bai, F. R. Brushett, and M. Z. Bazant, Sci. Rep. **6** (2016).
[17] A. Mani and M. Z. Bazant, Phys. Rev. E **84**, 061504 (2011).
[18] D. Deng, E. V. Dydek, J.-H. Han, S. Schlumpberger, A. Mani, B. Zaltzman, and M. Z. Bazant, Langmuir **29**, 16167 (2013).
[19] S. Schlumpberger, N. B. Lu, M. E. Suss, and M. Z. Bazant, Environ. Sci. Technol. Lett. **2**, 367 (2015).
[20] M. Z. Bazant, Phys. Rev. E **73**, 060601 (2006).
[21] C. H. Rycroft and M. Z. Bazant, Proc. R. Soc. A **472**, 20150531 (2016).
[22] C.-W. Park and G. Homsy, J. Fluid Mech. **139**, 291 (1984).
[23] B. J. Kirby and E. F. Hasselbrink, Electrophoresis **25**, 187 (2004).
[24] R. J. Hunter, *Zeta Potential in Colloid Science: Principles and Applications*, 3rd ed. (Academic Press, New York, 1988).
[25] W. B. Russel, D. A. Saville, and W. R. Schowalter, *Colloidal Dispersions* (Cambridge University Press, Cambridge, England, 1989); J. Lyklema, *Fundamentals of Interface and Colloid Science: Solid-Liquid Interfaces*, Fundamentals of Interface & Colloid Science, Vol. 2 (Academic Press, New York, 1995).
[26] L. Onsager, Phys. Rev. **37**, 405 (1931).
[27] M. Z. Bazant, Phys. Rev. Fluids **1**, 024001 (2016).
[28] S. R. De Groot and P. Mazur, *Non-Equilibrium Thermodynamics* (Interscience Publishers, New York, 2013).
[29] P. B. Peters, R. Van Roij, M. Z. Bazant, and P. M. Biesheuvel, Phys. Rev. E **93**, 053108 (2016).
[30] F. H. J. Van Der Heyden, D. J. Bonthuis, D. Stein, C. Meyer, and C. Dekker, Nano Lett. **6**, 2232 (2006); **7**, 1022 (2007).
[31] A. Guittet, M. Lepilliez, S. Tanguy, and F. Gibou, J. Comput. Phys. **298**, 747 (2015).
[32] S. Osher and J. Sethian, J. Comput. Phys. **79**, 12 (1988); S. Osher and R. Fedkiw, *Level Set Methods and Dynamic Implicit Surfaces*, Applied Mathematical Sciences Vol. 153 (Springer Science & Business Media, New York, 2006); J. A. Sethian, *Level Set Methods and Fast Marching Methods: Evolving Interfaces in Computational Geometry, Fluid Mechanics, Computer Vision, and Materials Science*, Cambridge Monographs on Applied and Computational Mathematics Vol. 3 (Cambridge University Press, Cambridge, England, 1999).
[33] C. Min and F. Gibou, J. Comput. Phys. **225**, 300 (2007).
[34] M. Mirzadeh, A. Guittet, C. Burstedde, and F. Gibou, J. Comput. Phys. **322**, 345 (2016).
[35] L. Paterson, J. Fluid Mech. **113**, 513 (1981).
[36] T. T. Al-Housseiny, P. A. Tsai, and H. A. Stone, Nat. Phys. **8**, 747 (2012); T. T. Al-Housseiny and H. A. Stone, Phys. Fluids **25**, 092102 (2013).

[37] I. Eames, M. Gilbertson, and M. Landeryou, J. Fluid Mech. **523**, 261 (2005).
[38] A. J. Pascall and T. M. Squires, J. Fluid Mech. **684**, 163 (2011).
[39] T. Robinson and I. Eames, J. Eng. Math. **103**, 77 (2017).
[40] J. R. Melcher and G. I. Taylor, Annu. Rev. Fluid Mech. **1**, 111 (1969); J. R. Melcher, Continuum Electromechanics (MIT Press, Cambridge, MA, 1981); J. R. Melcher, Field-Coupled Surface Waves (MIT Press, Cambridge, MA, 1963).
[41] G. I. Taylor and A. D. McEwan, J. Fluid Mech. **22**, 1 (1965).
[42] H. Lin, B. D. Storey, M. H. Oddy, C.-H. Chen, and J. G. Santiago, Phys. Fluids **16**, 1922 (2004); C.-H. Chen, H. Lin, S. K. Lele, and J. G. Santiago, J. Fluid Mech. **524**, 263 (2005).
[43] C. L. Druzgalski, M. B. Andersen, and A. Mani, Phys. Fluids **25**, 110804 (2013).
[44] H. Girault, Electrochim. Acta **32**, 383 (1987).
[45] M. Senda, T. Kakiuchi, and T. Osaka, Electrochim. Acta **36**, 253 (1991); H. H. Girault, in *Modern Aspects of Electrochemistry*, Vol. 25 (Plenum Press, New York, 1993); Z. Samec, Pure Appl. Chem. **76**, 383 (2004); H. H. Girault, Electroanal. Chem. **23**, 1 (2010).
[46] C. W. Monroe, L. I. Daikhin, M. Urbakh, and A. A. Kornyshev, Phys. Rev. Lett. **97**, 136102 (2006).
[47] J. B. Edel, A. A. Kornyshev, A. R. Kucernak, and M. Urbakh, Chem. Soc. Rev. **45**, 1581 (2016).
[48] R. F. Probstein and R. E. Hicks, Science **260**, 498 (1993); A. P. Shapiro and R. F. Probstein, Environ. Sci. Technol. **27**, 283 (1993).
[49] R. Lenormand, E. Touboul, and C. Zarcone, J. Fluid Mech. **189**, 165 (1988).
[50] B. Zhao, C. W. MacMinn, and R. Juanes, Proc. Natl. Acad. Sci. U.S.A. **113**, 10251 (2016).